PERGAMON

Vision Research 39 (1999) 3737–3744

Vision Research

www.elsevier.com/locate/visres

Discriminating mirror symmetry in foveal and extra-foveal vision

B.T. Barrett [a,*], D. Whitaker [a], P.V. McGraw [a], A.M. Herbert [b]

[a] *Department of Optometry, University of Bradford, Richmond Road, Bradford BD7 1DP, UK*
[b] *Ecole d'Optometrie, Universite de Montreal, C.P. 6128 Succursale Centre-Ville, Montreal, Que., Canada H3C 3J7*

Received 28 July 1998; received in revised form 5 April 1999

Abstract

The ability to discriminate perfect from imperfect mirror symmetry was examined at the fovea and at eccentricities out to 10° in the nasal visual field. A 2-AFC method of constant stimuli was employed in which a bilaterally symmetric pattern was presented in one interval and a degraded version of this symmetric pattern in the other. The subject's task was to decide which interval contained the perfectly symmetric pattern. Pattern size was varied by changing the viewing distance. Probit analysis revealed the degree of asymmetry corresponding to 75% correct performance. Given sufficient size scaling, perfectly symmetric stimuli can be discriminated from degraded symmetric stimuli in extra-foveal vision. Spatial scaling with an E_2 value similar to that for positional acuity was successful in removing the eccentricity dependence for the task. © 1999 Elsevier Science Ltd. All rights reserved.

Keywords: Symmetry; Spatial scaling; Periphery

1. Introduction

Performance on the vast majority of visual tasks is critically dependent upon visual field location. In general visual performance declines with increasing retinal eccentricity. The rate of decline with eccentricity has received considerable attention, and has been shown to be task dependent. For example, contrast sensitivity and resolution decline at a much slower rate with retinal eccentricity than does performance on positional acuity tasks (Levi, Klein & Aitsebaomo, 1985; Whitaker, Mäkelä, Rovamo, & Latham, 1992). Differences in the rate of decline with eccentricity between tasks are commonly expressed in terms of the parameter E_2 (Levi et al., 1985). The value of E_2 corresponds to the eccentricity at which the stimulus size must double in order to maintain foveal performance. In other words, once peripheral stimuli are spatially magnified by an appropriate amount, performance becomes equivalent across the visual field (Rovamo & Virsu, 1979) and differences between central and peripheral vision can be said to be quantitative rather than qualitative.

The ubiquitous nature of bilateral or mirror symmetry suggests an important role for this visual attribute (Tyler & Hardage, 1995; Wagemans, 1995; Gurnsey, Herbert & Kenemy, 1998). In humans, mirror symmetry is a salient visual property which, at least in central vision, is effortlessly and rapidly detected (for a review see Wagemans, 1995). This is particularly true of mirror symmetry about a vertical axis. In addition to being able to detect mirror symmetry, perfectly symmetric stimuli can be distinguished from degraded symmetric stimuli in central vision. Indeed, performance is equivalent on these two classes of symmetry task in foveal vision (Barlow & Reeves, 1979).

Although detection and discrimination of symmetry at the fovea have been studied extensively, performance on these tasks in extra-foveal vision has received comparatively little attention. This is rather surprising, given that the detection of symmetric forms against an asymmetric background in peripheral vision may be important for survival and locomotion (Tyler & Hardage, 1995; Gurnsey et al., 1998). It has been argued that the importance of symmetry detection is to aid in selecting targets for further visual processing, and therefore symmetry should be salient across the visual field. A number of studies have shown that symmetry

* Corresponding author. Fax: +1-274-385-570.
E-mail address: b.t.barrett@bradford.ac.uk (B.T. Barrett)

PII: S0042-6989(99)00083-8

detection is possible in extra-foveal vision (albeit with variably reduced performance when compared to performance at the fovea) (Barlow & Reeves, 1979; Masame, 1983; Herbert & Humphrey, 1996), but only a few studies have systematically examined symmetry detection as a function of retinal eccentricity. Furthermore, the ability to distinguish perfect symmetry from degraded symmetry has not been examined in peripheral vision.

Saarinen (1988) examined horizontal symmetry detection in the periphery using patterns scaled in size according to the cortical magnification factor derived from the sampling density of retinal ganglion cells (Virsu, Nasanen & Osmoviita, 1987). The decline in performance across the range of eccentricities tested was significantly reduced for the M-scaled patterns relative to the decline for the constant-sized patterns. However, size scaling the patterns in this manner did not equate foveal and peripheral performance.

Tyler and Hardage (1995) used a method of self-scaling to investigate vertical symmetry detection across the visual field where changes in stimulus size were achieved by changing the viewing distance. Thus, a halving of viewing distance resulted in a doubling of stimulus size and of stimulus eccentricity. The self-scaling method was successful in equating performance across most of the visual field. As outlined in Appendix A, the method of self-scaling can be expected to equate visual performance in peripheral vision if the eccentricities investigated are large relative to the E_2 for the task. By comparing their results for mirror symmetry detection with the fall off for resolution and positional acuity, Tyler and Hardage (1995) concluded that the amount of peripheral magnification required for symmetry detection was at least as great as that required for positional acuity. Thus, although symmetry detection for unscaled stimuli declines rapidly with retinal eccentricity, appropriate size scaling removes the eccentricity dependence.

In a recent study by Gurnsey et al. (1998) the rate of decline in symmetry detection across the visual field for vertically symmetric patches was estimated using a variant of the spatial scaling approach, in which a range of stimulus sizes were presented at each eccentricity. Usually, a threshold stimulus size is found at each eccentricity (including the fovea) and these data are used to determine the rate at which size must increase with eccentricity in order to maintain performance equivalent to that at the fovea. Gurnsey et al. adopted a somewhat different approach in that they determined eccentricity thresholds for each given stimulus size. Whilst this should be equivalent to a conventional spatial scaling method it does have the disadvantage that no estimate of foveal performance is obtained, necessitating critical extrapolation in order to quantify the eccentricity dependence of the task. Gurnsey et al. (1998) suggest that the eccentricity dependent decline for detecting symmetry in patches presented in isolation is more exaggerated than for resolution but slower than that for positional acuity.

In the present study we use a conventional spatial scaling technique (Watson, 1987) in order to determine whether perfect symmetry can be discriminated from imperfect symmetry in extra-foveal vision and, if so, to quantify the dependence of this task upon retinal eccentricity.

2. Methods

2.1. Stimuli

Generation and control of stimuli were performed using the macro capabilities of the public domain software NIH Image™ 1.59 (developed at the US National Institutes of Health and available from the Internet by anonymous FTP from zippy.nimh.nih.gov or on floppy disk from the National Technical Information Service, Springfield, Virginia, part number PB95-500195GEI). Stimuli were presented on an Electron D2 21-inch CRT with a mean luminance of 32.7 cd m^{-2} and a frame rate of 75 Hz. The non-linear luminance response of the display was linearised by using the inverse function response as measured with a Minolta CS-100 photometer. Contrast resolution of up to 12-bit accuracy was obtained by combining the red, green and blue outputs of the video board using a video summation device constructed according to Pelli and Zhang (1991). The host computer was a Motorola StarMax 4000/200.

Sample patterns are shown in Fig. 1. The patterns were constructed by randomly assigning one of 256 grey levels to each 2×2 pixel block (Fig. 1a) or 4×4 pixel block (Fig. 1d) in the left half of the stimulus window. Symmetry was generated by reflecting the positions of the blocks in this half-pattern across a vertical axis such that the axis of the pattern was itself only one block wide (Figs. 1a and d). Each symmetric pattern was then subjected to five different levels of asymmetric degradation. Degradation was introduced by assigning a new random grey level to a known proportion of the 2×2 or 4×4 pixel blocks across the pattern. Starting with the symmetric pattern in each case, greater levels of asymmetry were created by doubling the proportion of blocks whose grey level was to change in successive patterns. Once the stimuli had been created and subjected to different levels of asymmetric degradation, the patterns were windowed in contrast by a two-dimensional Gaussian with a standard deviation of 33 pixels.

Figure 1b and e show examples of the asymmetric degradation for the 2×2 pixel block and 4×4 pixel block stimuli, respectively. In both cases the patterns

are asymmetric to the extent that approximately 10% of the blocks have been subjected to a change in grey level by comparison with the perfectly symmetric patterns. Figure 1c and f show examples of asymmetric patterns where approximately 40% of the blocks have randomly altered grey levels.

For each block size, a total of 60 stimuli were used in the experiment, comprising ten symmetric patterns each with five fellow patterns containing differing degrees of asymmetric degradation. Stimuli were randomly chosen from any one of these ten stimulus sets in order to reduce the possibility of chance stimulus arrangements distorting results. Prior to data collection contrast detection thresholds were determined for the stimuli under each viewing condition using a yes/no staircase procedure. All subsequent stimulus presentations were maintained at four-times detection threshold. This value represented the maximum contrast for which complete data sets could be obtained for the range of eccentricities tested.

2.2. Subjects

Two of the authors acted as subjects (BTB and DW). Both underwent extensive practice prior to data collection. Subjects viewed the screen monocularly and wore optimal distance correction. Data were collected under conditions of dim room illumination.

2.3. Procedure

On any given trial, two 150 ms presentations were made, separated by an inter-stimulus interval of 500 ms. One interval contained a symmetric pattern, while the other interval contained one of the five degraded versions of this pattern. The observer was required to indicate which interval contained the perfectly symmetric pattern. The order of presentation was randomised and the procedure continued for a total of 150 trials, with each of the five levels of asymmetry presented on 30 trials. No feedback was provided. The procedure was carried out for foveal viewing and for eccentricities of 2.5, 5, 7.5 and 10° in the nasal visual field. Eccentricity was measured from a fixation point to the centre of the pattern. No fixation point was present for the foveal condition. At any given eccentricity, a range of pattern sizes (quantified by the angular subtense of the Gaussian contrast window) was obtained by changing the viewing distance. For each eccentricity/pattern size combination, thresholds were determined from three separate runs, making a total of 90 observations per point. The results were analysed by probit analysis to reveal the degree of asymmetry corresponding to 75% correct discrimination in the symmetric versus degraded-symmetric task.

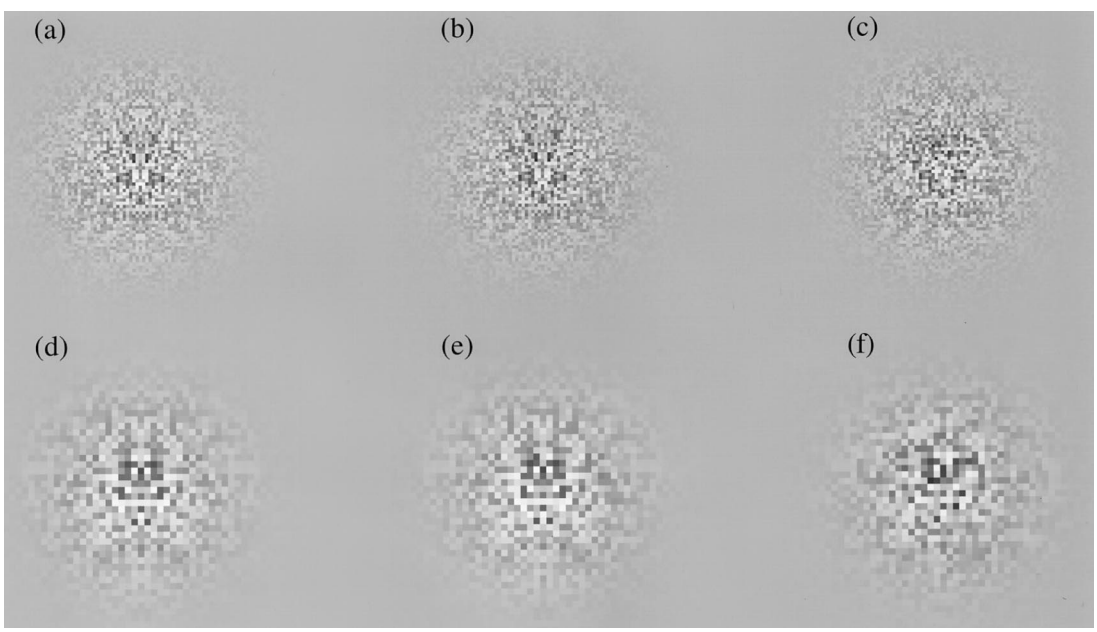

Fig. 1. Examples of the stimuli used in the present experiment (upper panels 2×2 pixel block patterns; lower panels 4×4 pixel block patterns). Pattern (a) is 100% bilaterally symmetric about a vertical axis. Patterns (b) and (c) are asymmetrically degraded versions of pattern (a) where 10 and 40% of the blocks, respectively have been subjected to a random change in grey level. Patterns (d)–(f) show equivalent sample patterns for the 4×4 pixel block stimuli.

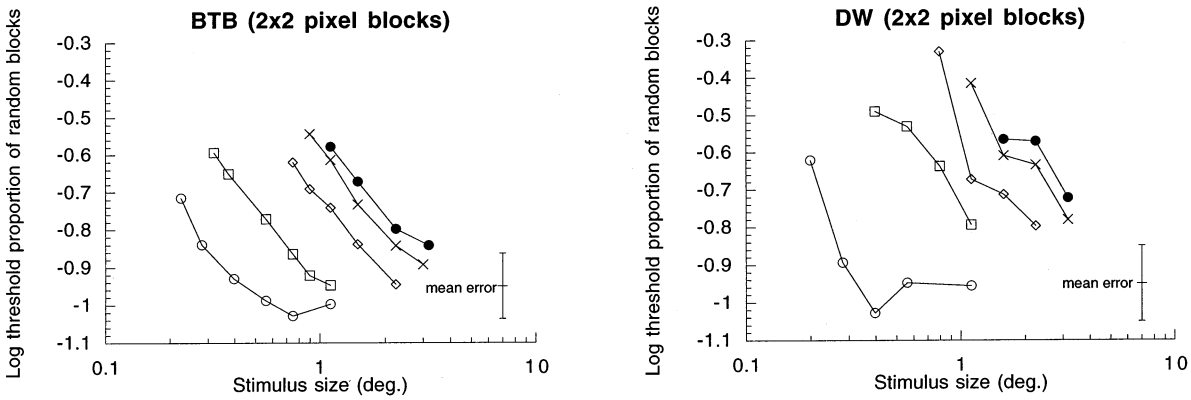

Fig. 2. Proportion of random blocks corresponding to 75% correct responses in the 2×2 pixel block symmetric versus degraded-symmetry task plotted as a function of the angular subtense of the standard deviation of the Gaussian window applied to the patterns. Results are shown for subjects BTB (left panel) and DW (right panel). Angular size was altered by changing the viewing distance. Performance is shown for four eccentricities 0° (○), 2.5° (□), 5° (◇), 7.5° (X) and 10° (●). The mean standard error is shown.

3. Results

Figure 2 shows the proportion of random blocks necessary to obtain 75% correct discrimination between the symmetric and degraded-symmetric stimuli plotted as a function of the stimulus size (the angular subtense of the standard deviation of the Gaussian) for the 2×2 pixel block condition. The functions for the two subjects show the same general shape for foveal viewing. Performance improves as the patch size is increased and then becomes asymptotic at around 10% (log threshold proportion $= -1$) as the pattern width is further increased. Data for the extra-foveal viewing conditions show a steep improvement in performance similar to that observed for the foveal condition but do not exhibit an asymptotic portion. This is because the requirement for greater stimulus magnification becomes so large in extra-foveal vision that the stimuli begin to overlap the fovea. The data of subject BTB exhibit better extra-foveal performance than those of subject DW. Figure 3 shows data for the 4×4 pixel block condition. The data in these figures show a similar trend to the 2×2 pixel condition with the exception of the fact that the functions are shifted leftwards along the size axis relative to the functions observed for the 2×2 pixel block condition (Fig. 2). This implies that performance becomes asymptotic at smaller stimulus sizes as compared with the 2×2 pixel block condition, allowing us to see the start of an asymptotic level of performance for the extra-foveal data, at least at small eccentricities. Again, subject DW shows a more rapid loss of performance with decreasing stimulus size in extra-foveal vision. For both subjects, however, optimal extra-foveal performance reaches a level similar to that at the fovea.

We now model the data in terms of both internal limiting noise factors and an eccentricity-dependent scaling factor. We adopt the view that, at any eccentricity, discrimination of symmetric versus degraded symmetric stimuli cannot be achieved until the external stimulus distortion exceeds the level of intrinsic noise. We assume that intrinsic noise arises from two uncorrelated sources, one which is independent of stimulus size (σ_i) and one which is inversely dependent upon stimulus size (σ_d). For example, white spatiotemporal neural noise (Pelli, 1991) would be expected to decrease with stimulus size through a process of averaging across space. The effects of other potential sources of noise, such as spatial undersampling or intrinsic topographic disorder (jitter) of neural receptive fields, depend upon their implementation. For example, positional jitter can either be modelled as being of fixed spatial extent, or it can be considered in a scale-invariant manner, in which the jitter is a constant fraction of filter size (Hess, Field & Watt, 1990). In a similar way, Wang, Levi and Klein (1996) modelled the task of bisection acuity using a combination of uncorrelated intrinsic noise sources.

Along the lines described above, discrimination thresholds depend upon a combination of two noise sources

$$T = k\sqrt{\sigma_i^2 + \sigma_d^2}$$

or

$$T = k\sqrt{\sigma_i^2 + \left(\frac{k'}{\text{size}}\right)^2} \quad (1)$$

where k' is the constant of proportionality relating the size-dependent noise source to the inverse of stimulus size.

This equation therefore predicts two regions, one at large stimulus sizes, where threshold becomes optimal and independent of size

$$T = T_{\text{opt}} = k\sigma_i \quad (2)$$

and one at small sizes where threshold is inversely proportional to size

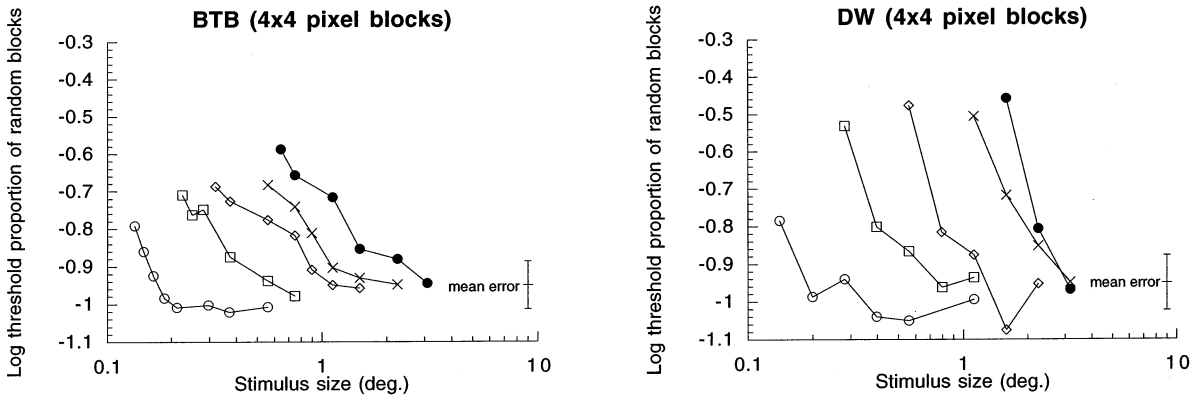

Fig. 3. As for Fig. 2, but for 4×4 pixel block condition. The mean standard error is shown.

$$T = \frac{kk'}{\text{size}}$$

From Eq. (1), the transition between these two regions can be seen to occur when

$$\sigma_i = \frac{k'}{\text{size}} \quad \text{i.e.} \quad k' = \sigma_\text{i}\,\text{size}_\text{trans} \tag{3}$$

Substituting into Eq. (1), we have

$$T = k\sqrt{\sigma_\text{i}^2 + \left(\frac{\sigma_i\,\text{size}_\text{trans}}{\text{size}}\right)^2} = k\sigma_\text{i}\sqrt{1 + \frac{\text{size}_\text{trans}}{\text{size}}}$$
$$= T_\text{opt}\sqrt{1 + \frac{\text{size}_\text{trans}}{\text{size}}} \tag{4}$$

by substitution of Eq. (2).

Finally, we take into account the change of scale of the visual system with increasing eccentricity. The most widely used relationship states that extra-foveal scale increases from a finite value at the fovea as a linearly varying function of eccentricity, E. At any eccentricity, Eq. (4) then becomes

$$T = T_\text{opt}\sqrt{1 + \left(\frac{\text{size}_\text{trans}}{\text{size}*(1 + (E/E_2))}\right)}$$

where E_2 is a constant describing the rate of change in scale as a function of eccentricity. Taking the log of both sides we have

$$\log T = \log\left[T_\text{opt}\sqrt{1 + \left(\frac{\text{size}_\text{trans}}{\text{size}*(1 + (E/E_2))}\right)}\right] \tag{5}$$

For each observer, Eq. (5) was applied to the data sets shown in Figs. 2 and 3. A value of E_2 was chosen on the basis of visual inspection of the data, and the residual sum of squares of the data from Eq. (5) was calculated. An iterative procedure was then adopted to find the E_2 value which minimised the residual sum of squares deviations.

This procedure has the effect that data from different eccentricities collapse together (Figs. 4 and 5), indicating that discrimination of perfect from imperfect symmetry in foveal and extra-foveal vision can be equated simply by a change of scale. The exception to this rule is BTB's 2×2 data for 2.5° eccentricity which appear to have been overcorrected by the scaling procedure. A non-linear accelerating scaling function would therefore be expected to improve the proportion of variance explained for this data set, but we present the linearly-scaled data for simplicity. Functions fitted to the data in Figs. 4 and 5 represent the best-fitting versions of Eq. (5). Parameters resulting from the curve fitting procedure are shown in Table 1.

Values of T_opt, the asymptotic level of performance at large sizes, demonstrate that discrimination of symmetric versus non-symmetric stimuli can only be performed across the visual field once the percentage of randomised blocks approaches 10%. Values of size_trans, the scaled stimulus size representing the transition between the flat and ascending limbs of the function, are seen to be approximately twice as large for the 2×2 pixel block condition compared with the 4×4 pixel block condition (Table 1).

4. Discussion

Most previous investigations of human mirror symmetry have employed a task which requires subjects to distinguish perfectly symmetric patterns from wholly random patterns. Several previous studies have reported that mirror symmetry detection is possible in extra-foveal vision but with reduced sensitivity when compared to the fovea (Barlow & Reeves, 1979; Masame, 1983; Saarinen, 1988; Herbert & Humphrey, 1996), but no study has previously examined whether perfectly symmetric stimuli can be distinguished from degraded symmetric patterns in extra-foveal vision. The results of the present investigation indicate that the latter task is possible when the axis of symmetry is centered away from fixation, although stimuli require substantial levels of magnification in extra-foveal vision. The results are, therefore, in support of the view

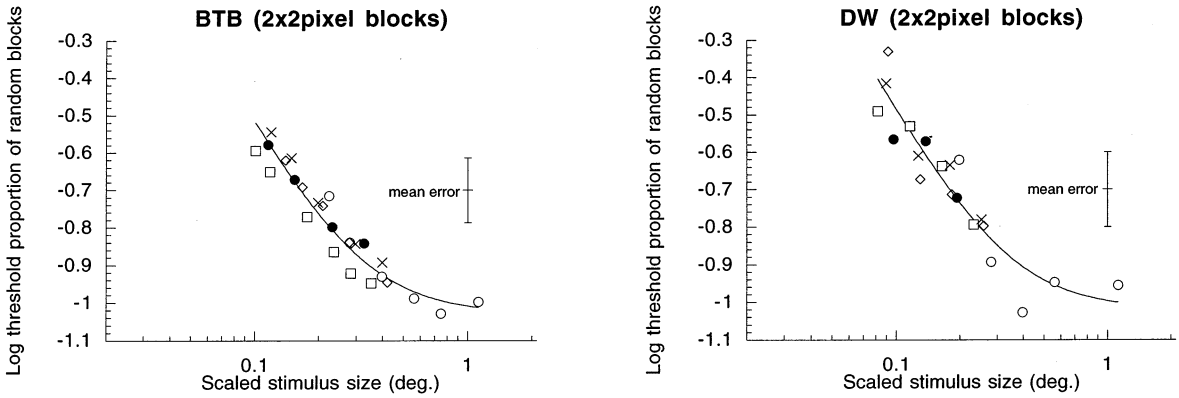

Fig. 4. The data of Fig. 2 has been scaled according to the best-fitting version of Eq. (5), depicted by the solid curve. Parameters resulting from this curve fitting procedure are shown in Table 1. Symbols are as in Fig. 2. See text for details.

that performance on tasks involving symmetry at the fovea and periphery differ quantitatively rather than qualitatively (Tyler & Hardage, 1995; Gurnsey et al., 1998). Spatial scaling with an E_2 value of between 0.57° (subject DW) and 1.15° (subject BTB) was successful in removing the eccentricity dependence for the task. In the study by Saarinen (1988) the peripheral stimuli were spatially scaled according to Rovamo and Virsu's (1979) cortical magnification factor whose equivalent E_2 value is about 3°. This is substantially greater than that found in the present study. Our results suggest that foveal and peripheral performance were not fully equated in Saarinen's (1988) investigation because of insufficient magnification of the peripherally presented stimuli.

Two recent studies have examined mirror symmetry detection as a function of retinal eccentricity. Tyler and Hardage (1995) examined the effect of exposure duration upon symmetry detection for stimulus pairs separated across a horizontal or vertical midline. They found that self-scaling of their stimuli beyond 2° eccentricity was successful in equating performance across the visual field. As outlined in Appendix A, self-scaling is equivalent to the spatial scaling used in the present study provided the eccentricities examined are large relative to the E_2 values for the task. Given the small E_2 values found here ($\approx 0.8°$), even at an eccentricity as small as 2°, magnification predictions from self-scaling (Appendix A, Eq. (8)) and spatial scaling (Appendix A, Eq. (7)) differ by 40%. At smaller eccentricities, however, the discrepancy begins to accelerate, and symmetry performance using self-scaled stimuli deteriorates rapidly (Tyler & Hardage, 1995). By showing that the reduction in sensitivity for their symmetry task agreed with the predicted decline in positional acuity, but not resolution acuity, Tyler & Hardage provided an estimate of the magnification function for both local and long range symmetry detection, an estimate which the present results confirm.

Gurnsey et al. (1998) also measured the effect of retinal eccentricity upon mirror symmetry detection. They measured eccentricity thresholds for symmetry identification at four different stimulus sizes. Whilst the method adopted by Gurnsey et al. did not provide a measure of foveal performance, the authors were able to estimate the value of E_2 for their task. They suggested that the E_2 value for their isolated symmetry condition (the condition which most closely resembles the stimuli employed in the present study) would be in the region of 1.2°. This is somewhat larger than the value derived from the present results for subject DW but is in reasonable agreement with the results for subject BTB. The present results, taken together with those from previous investigations of mirror symmetry in the periphery (Saarinen, 1988; Tyler and Hardage, 1995; Gurnsey et al., 1998), therefore support the view that detection and discrimination of mirror symmetry falls at a faster rate with eccentricity than resolution, but at a rate which is comparable to positional acuity (Levi et al., 1985).

A comparison of the results reveals a difference in the overall patch size for the 2×2 and 4×4 pixel block conditions above which performance becomes asymptotic ($size_{trans}$ in Table 1). This argues against a fixed, critical patch size which is independent of spatial frequency content of the pattern and above which performance becomes asymptotic (Jenkins, 1982). Recently, Dakin and Herbert (1998) showed that the critical patch size varies inversely with spatial frequency. Due to the broadband nature of the patterns employed in the present experiment it is not possible to draw any firm conclusion concerning the influence of spatial frequency content upon task performance. However, the fact that the scaled stimulus size representing the transition between the flat and ascending limbs of the function ($size_{trans}$) is approximately twice as large for the 2×2 pixel block condition compared with the 4×4 pixel block condition (Table 1) suggests that it is the

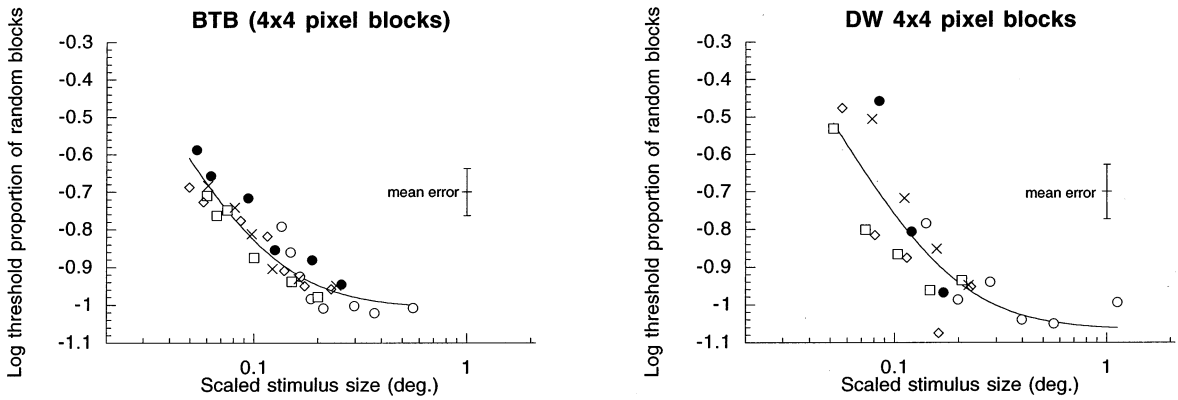

Fig. 5. The data of Fig. 3 has been scaled according to the best-fitting version of Eq. (5), depicted by the solid curve. Parameters resulting from this curve fitting procedure are shown in Table 1. Symbols are as in Fig. 3. See text for details.

size of the pixel blocks which are the decisive factor in determining performance rather than the size of the Gaussian contrast window. This conclusion is consistent with the appearance of the stimuli (Fig. 1), in which the patch size is always large relative to the size of the pattern within it.

The effect of eccentricity upon visual performance is known to be extremely task dependent. For example, the ability to identify movement or to detect the presence of objects defined by luminance varies only gradually across the visual field, with relatively little peripheral stimulus magnification needed in order to become comparable with foveal performance levels (Whitaker et al., 1992; Latham, Whitaker, Wild & Elliott, 1993). Other tasks, such as those which involve the analysis of the relative position of objects, require much greater levels of magnification in the periphery in order to equate performance with that at the fovea (e.g. Levi et al., 1985; Whitaker et al., 1992). This range of task-dependent scaling factors is obviously less satisfactory than the simple situation in which a single factor equates performance across eccentricity for all tasks (Virsu & Rovamo, 1979). Further discussions of this topic and investigations into its possible origins have been reported elsewhere (Drasdo, 1991; Wilson, 1991; Whitaker et al., 1992; Mäkelä, Rovamo & Whitaker, 1997; Beard, Levi & Klein, 1997). The present study reveals that eccentricity dependent differences in performance on the task of detecting mirror symmetry or signalling minor deviations from perfect symmetry can be eliminated by spatially scaling the stimulus by an amount equivalent to that required for positional tasks (Levi et al., 1985). In other words, the neural resources required for symmetry discrimination are available across the visual field and exhibit similar levels of performance once sufficient stimulus magnification is provided.

Table 1
Parameters of the curve fitting procedure (Eq. (5)) for the 2×2 and 4×4 pixel block conditions[a]

		BTB	DW
E_2[b] (°)	2×2 Pixel blocks	1.15 ± 0.14	0.65 ± 0.11
	4×4 Pixel blocks	0.91 ± 0.15	0.57 ± 0.19
T_{opt}[c] (%)	2×2 Pixel blocks	9.4 ± 1	9.6 ± 1.1
	4×4 Pixel blocks	9.8 ± 0.37	8.6 ± 1.0
$Size_{trans}$[d] (°)	2×2 Pixel blocks	0.309 ± 0.026	0.326 ± 0.049
	4×4 Pixel blocks	0.114 ± 0.008	0.176 ± 0.034
Variance explained (%)	2×2 Pixel blocks	91.7	87.3
	4×4 Pixel blocks	87.1	71.6

[a] Errors represent ±1 S.D. either side of the parameter value. See text for further details.
[b] E_2, eccentricity at which the stimulus size must double to maintain foveal performance.
[c] T_{opt}, optimum performance level.
[d] $Size_{trans}$, scaled stimulus size which represents the transition between the flat and ascending potions of the curve-fit.

Acknowledgements

BTB is supported by a Research Development Grant from the Wellcome Trust. PVM is supported by a Vision Research Training Fellowship from the Wellcome Trust.

Appendix A. Self-scaling versus spatial scaling

In the method of self-scaling, stimulus size is doubled with each doubling of eccentricity. Stimulus size at any eccentricity is thus given by

$$k^*E \tag{6}$$

where k is a constant. Stimulus size falls to zero when eccentricity is zero, implying an infinite foveal resource dedicated to task performance.

In the method of spatial scaling, stimulus size and eccentricity are related by

$$k'^* \ (1 + (E/E_2)) \tag{7}$$

where E_2 represents the eccentricity at which the finite foveal stimulus size (k') needs to double in order to maintain performance.When $((E/E_2) \gg 1)$, Eq. (2) approximates to

$$k'^*(E/E_2) \tag{8}$$

which can be seen to be equivalent to Eq. (1) with a relationship between the constants of $k = k'/E_2$.Thus, when $(E/E_2) \gg 1$ (i.e. when eccentricity is large relative to E_2), the method of self-scaling and spatial scaling become equivalent. Self-scaling would therefore be expected to equate visual performance in peripheral vision provided the eccentricities investigated are large relative to the E_2 for the task.

References

Barlow, H. B., & Reeves, B. C. (1979). The versatility and absolute efficiency of detecting mirror symmetry in random dot displays. *Vision Research*, *19*, 783–793.

Beard, B. L., Levi, D. M., & Klein, S. A. (1997). Vernier acuity with non-simultaneous targets: the cortical magnification factor estimated by psychophysics. *Vision Research*, *37*, 325–346.

Dakin, S. C., & Herbert, A. M. (1998). The spatial region of integration for visual symmetry detection. *Proceedings of the Royal Society of London* (*B*), *265*, 659–664.

Drasdo, N. (1991). Neural substrates and threshold gradients in peripheral vision. In J. R. Cronly-Dillon, *Vision and visual dysfunction*. Basingstoke, UK: Macmillan.

Gurnsey, R., Herbert, A. M., & Kenemy, J. (1998). Bilateral symmetry embedded in noise is detected accurately only at fixation. *Vision Research*, *38*, 3795–3803.

Herbert, A. M., & Humphrey, G. K. (1996). Bilateral symmetry detection: testing a callosal hypothesis. *Perception*, *25*, 463–480.

Hess, R. F., Field, D., & Watt, R. J. (1990). The puzzle of amblyopia. In C. Blakemore, *Vision: coding and efficiency*. Cambridge: Cambridge University Press.

Jenkins, B. (1982). Redundancy in the perception of bilateral symmetry in dot textures. *Perception and Psychophysics*, *32*, 171–177.

Latham, K., Whitaker, D., Wild, J. M., & Elliott, D. B. (1993). Magnification perimetry. *Investigative Ophthalmology & Visual Science*, *34*, 1691–1701.

Levi, D. M., Klein, S. A., & Aitsebaomo, A. P. (1985). Vernier acuity, crowding and cortical magnification. *Vision Research*, *25*, 963–977.

Mäkelä, P., Rovamo, J., & Whitaker, D. (1997). The effects of eccentricity and stimulus magnification on simultaneous performance in position and movement acuity tasks. *Vision Research*, *37*, 1261–1270.

Masame, K. (1983). Detection of symmetry in complex patterns: does symmetric projection to the visual system necessary for the projection of symmetry? *Tohoku Psychol Folia*, *42*, 27–33.

Pelli, D. G. (1991). The quantum efficiency of human vision. In C. Blakemore, *Vision: coding and efficiency*. Cambridge: Cambridge University Press.

Pelli, D. G., & Zhang, L. (1991). Accurate control of contrast on microcomputer displays. *Vision Research*, *31*, 1337–1350.

Rovamo, J., & Virsu, V. (1979). An estimation and application of the human magnification factor. *Experimental Brain Research*, *37*, 495–510.

Saarinen, J. (1988). Detection of mirror symmetry in random dot patterns at different eccentricities. *Vision Research*, *28*, 755–759.

Tyler, C. W., & Hardage, L. (1995). Mirror symmetry detection: predominance of second-order pattern processing throughout the visual field. In C. W. Tyler, *Human symmetry perception and its computational analysis* (pp. 151–171). Utrecht: VSP Publishers.

Virsu, V., & Rovamo, J. (1979). Visual resolution, contrast sensitivity, and the cortical magnification factor. *Experimental Brain Research*, *37*, 475–494.

Virsu, V., Nasanen, R., & Osmoviita, K. (1987). Cortical magnification and peripheral vision. *Journal of the Optical Society of America A*, *4*, 1568–1578.

Wagemans, J. (1995). Detection of visual symmetries. In C. W. Tyler, *Human symmetry perception and its computational analysis* (pp. 9–32). Utrecht: VSP Publishers.

Wang, H., Levi, D. M., & Klein, S. A. (1996). Intrinsic uncertainty and integration efficiency in bisection acuity. *Vision Research*, *36*, 717–739.

Watson, A. B. (1987). Estimation of local spatial scale. *Journal of the Optical Society of America A*, *4*, 1579–1582.

Whitaker, D., Mäkelä, P., Rovamo, J., & Latham, K. (1992). The influence of eccentricity on position and movement acuities as revealed by spatial scaling. *Vision Research*, *32*, 1913–1930.

Wilson, H. R. (1991). Model of peripheral and amblyopic hyperacuity. *Vision Research*, *31*, 967–982.